energies

MDPI

Article

Reorientation of Magnetic Graphene Oxide Nanosheets in Crosslinked Quaternized Polyvinyl Alcohol as Effective Solid Electrolyte

Jia-Shuin Lin [1], Wei-Ting Ma [1], Chao-Ming Shih [1], Bor-Chern Yu [1], Li-Wei Teng [1], Yi-Chun Wang [1], Kong-Wei Cheng [1,2], Fang-Chyou Chiu [1,3] and Shingjiang Jessie Lue [1,4,5,*]

1 Department of Chemical and Materials Engineering, and Green Technology Research Center, Chang Gung University, Kwei-shan, Taoyuan 333, Taiwan; ninalin99@gmail.com (J.-S.L.); carherine81@gmail.com (W.-T.M.); nanochitosan@gmail.com (C.-M.S.); z22622003@hotmail.com (B.-C.Y.); xz80919@hotmail.com.tw (L.-W.T.); peteryvonne110@hotmail.com (Y.-C.W.); kwcheng@mail.cgu.edu.tw (K.-W.C.); maxson@mail.cgu.edu.tw (F.-C.C.)

2 Department of Orthopaedic Surgery, Chang Gung Memorial Hospital, Keelung Branch, Taoyuan 333, Taiwan

3 Department of General Dentistry, Chang Gung Memorial Hospital, Taoyuan 333, Taiwan

4 Department of Radiation Oncology, Chang Gung Memorial Hospital, Taoyuan 333, Taiwan

5 Department of Safety, Health and Environmental Engineering, Ming-Chi University of Technology, New Taipei City 243, Taiwan

* Correspondence: jessie@mail.cgu.edu.tw; Tel.: +886-3-211-8800 (ext. 5489); Fax: +886-3-211-8700

Academic Editor: Haolin Tang

Received: 11 August 2016; Accepted: 14 November 2016; Published: 29 November 2016

Abstract: This work aims to clarify the effect of magnetic graphene oxide (GO) reorientation in a polymer matrix on the ionic conduction and methanol barrier properties of nanocomposite membrane electrolytes. Magnetic iron oxide (Fe_3O_4) nanoparticles were prepared and dispersed on GO nanosheets (GO-Fe_3O_4). The magnetic GO-Fe_3O_4 was imbedded into a quaternized polyvinyl alcohol (QPVA) matrix and crosslinked (CL-) with glutaraldehyde (GA) to obtain a polymeric nanocomposite. A magnetic field was applied in the through-plane direction during the drying and film formation steps. The CL-QPVA/GO-Fe_3O_4 nanocomposite membranes were doped with an alkali to obtain hydroxide-conducting electrolytes for direct methanol alkaline fuel cell (DMAFC) applications. The magnetic field-reoriented CL-QPVA/GO-Fe_3O_4 electrolyte demonstrated higher conductivity and lower methanol permeability than the unoriented CL-QPVA/GO-Fe_3O_4 membrane or the CL-QPVA film. The reoriented CL-QPVA/GO-Fe_3O_4 nanocomposite was used as the electrolyte in a DMAFC and resulted in a maximum power density of 55.4 mW·cm^{-2} at 60 °C, which is 73.7% higher than that of the composite without the magnetic field treatment (31.9 mW·cm^{-2}). In contrast, the DMAFC using the CL-QPVA electrolyte generated only 22.4 mW·cm^{-2}. This research proved the surprising benefits of magnetic-field-assisted orientation of GO-Fe_3O_4 in facilitating the ion conduction of a polymeric electrolyte.

Keywords: graphene oxide-iron oxide (GO-Fe_3O_4); crosslinked quaternized polyvinyl alcohol (CL-QPVA); magnetic field; reorientation; direct methanol alkaline fuel cell (DMAFC)

1. Introduction

Fuel cells convert chemical energy into electrical energy and are considered an alternative power supply [1]. Among the different types of fuel cells, direct methanol fuel cells (DMFCs) have obtained considerable attention because of their easy re-fuelling, high energy density, small size and low emissions of pollutants [2]. Moreover, DMFCs can be used in a variety of portable applications, such as laptops, cell phones and digital cameras [3]. Alkaline fuel cells using anion-exchange membranes

(such as Tokuyama A210) [4–6] or hydroxide-conducting membranes [7–9] provide advantages over proton-exchange membranes (PEMs), such as lower-cost membranes, reduced methanol cross-over, easy water management, and non-platinum catalyst [10–12].

Several nanofillers have been blended into membrane electrolytes to enhance the ionic conductivity. Huang et al. fabricated a polyvinyl alcohol (PVA) composite containing modified carbon nanotubes (m-CNTs) and showed that PVA/m-CNTs doped with 6 M potassium hydroxide (KOH) had a conductivity value 51.9% higher than that of PVA [13]. Lue et al. [14] incorporated fumed silica (FS) into a PVA membrane and formed a PVA/20% FS composite. The membrane had a higher conductivity than PVA (0.058 $S{\cdot}cm^{-1}$ vs. 0.018 $S{\cdot}cm^{-1}$, respectively). Yang et al. [15] prepared a quaternized polyvinyl alcohol/alumina (QPVA/Al_2O_3) nanocomposite polymer membrane and the membrane had an excellent electrochemical performance compared with pristine QPVA. In our previous publications, we decorated graphene oxide-iron oxide (GO-Fe_3O_4) on QPVA polymer to form an electrolyte membrane. The QPVA/GO-Fe_3O_4 membrane had better cell performance (172 $mA{\cdot}cm^{-2}$ vs. 51 $mA{\cdot}cm^{-2}$) and conductivity (0.0305 $S{\cdot}cm^{-1}$ vs. 0.0159 $S{\cdot}cm^{-1}$) over pristine QPVA [16]. Membranes incorporating nanofiller can increase the polymer free volume, and this might increase the ionic diffusivity within the membranes, which further enhances conductivity [17].

Many nanofillers in polymeric membranes can suppress methanol crossover in DMFCs. For example, iron oxide (Fe_3O_4) decorated CNTs in PVA membrane showed decreased methanol permeability [10]. Yuan et al. [18] layered poly(diallyldimethylammonium chloride) (PDDA) and GO nanosheets onto the surface of Nafion membrane. The methanol permeation across the composite membrane decreased in comparison to the pristine Nafion. Yang et al. [19] fabricated PVA/TiO_2 membranes with a permeability values of the order of 10^{-8} $cm^2{\cdot}s^{-1}$, which is one order of magnitude smaller than that of a PVA membrane.

Recently, GO has gained substantial attention for its noticeable thermal [20], mechanical and barrier properties [21]. GO is exfoliated from graphite [22–25] and it has been used in many applications, including supercapacitors [26], water treatment [27], Li ion batteries [28], and fuel cells [29–35]. Nair et al. [21] and Paneri et al. [36] proved that GO membranes can successfully block methanol, ethanol and hexane permeation while allowing water diffusion. Lin and Lu [37] reported that the methanol permeability of hot-pressed Nafion-GO decreased 41% relative to the pristine Nafion. Yuan et al. [18] reported that a GO-coating on a Nafion membrane lowered its methanol permeability. This indicates that GO can suppress alcohol crossover in membranes. However, some researchers indicate that the addition of GO filler decreased the composite's conductivity [22,37,38], whereas some determined that GO could increase the ion conductivity [39].

In our previous work, QPVA membranes were fabricated and applied in a direct methanol alkaline fuel cell (DMAFC) as membrane electrolytes [5,40]. With the introduction of quaternary ammonium groups (-$N^+(CH_3)_3$) onto the PVA matrix, QPVA exhibits anion-exchange functional groups [40] and better conductivity than pristine PVA [15]. These functional groups facilitate hydroxide ion (OH^-) transport through the membrane via the Grotthuss mechanism [41]. We also demonstrated that KOH-doped QPVA possessed excellent chemical stability in the Fenton test and maintained a high open circuit voltage (OCV) in a long-term DMAFC test (~230 h) [40].

Controlling the GO orientation in the polymer matrices is critical for better methanol suppression through increase of the apparent aspect ratio of the GO [22]. Reducing the methanol permeability directly lowers the cell over-potential and improves the cell voltage and power density [42]. With the objective of decreasing methanol crossover and improving conductivity, we prepared a well-aligned, CL-QPVA/GO-Fe_3O_4 membrane using an external magnetic field. Magnetic Fe_3O_4 nanoparticles were decorated onto GO nanosheets (GO-Fe_3O_4). Guo et al. [43] reported that ultrafiltration (UF) membranes containing magnetic particles were prepared with a magnetic field and demonstrated that this magnetic-field-assisted orientation can be achieved at an industrial scale. The resulting GO-Fe_3O_4 nanofillers were blended with QPVA polymer solution and cast into films. A magnetic field was applied to re-orient the nanofillers before the membranes solidified. To improve the stability of the

QPVA membranes in aqueous solutions, glutaraldehyde (GA) was used as a crosslinking reagent to reinforce the membrane integrity [44]. The three types of membranes (CL-QPVA, QPVA/GO-Fe_3O_4 nanocomposite membranes prepared with the magnetic field and QPVA/GO-Fe_3O_4 nanocomposite membranes prepared without the magnetic field) were tested for DMAFC performance. The chemical and physical characteristics of the membranes were also investigated and correlated to cell performance in this study.

2. Results and Discussion

2.1. Stability of Crosslinked Quaternized Polyvinyl Alcohol Membrane

QPVA is a water-soluble synthetic polymer. To maintain QPVA membrane stability in hot water, we used two different methods to form the crosslinked membranes, the pre-cross-linking (pre-CL) and post-cross-linking (post-CL) methods. The weight losses of the pre-CL membrane and the post-CL membranes are shown in Figure 1. This indicates that the post-CL membrane with 3 h crosslinking time demonstrated the least weight loss among the tested membranes. Hence, the following results are based on the samples with 3 h crosslinking time and denoted as CL-QPVA.

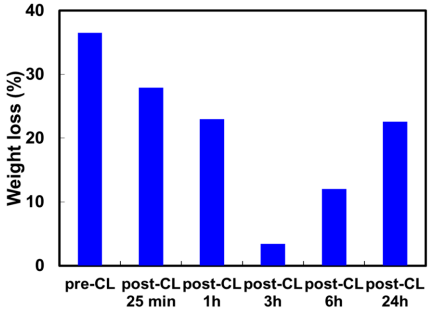

Figure 1. Dissolution of crosslinked quaternized polyvinyl alcohol (CL-QPVA) in 60 °C. The crosslinker was incorporated before (pre-cross-linking (pre-CL)) or after (post-cross-linking (post-CL)) the films were dried. The crosslink times of the post-CL samples are indicated.

2.2. Crystallinity and Mechanical Properties of Quaternized Polyvinyl Alcohol and Nanocomposite Membrane

PVA is a semi-crystalline polymer [14,40] and QPVA retained much of the PVA structure. The X-ray diffraction (XRD) patterns of the GO, Fe_3O_4, GO-Fe_3O_4, CL-QPVA, and un-aligned CL-QPVA/GO-Fe_3O_4 are shown in Figure 2a. The XRD band at 2θ of 11° corresponds to the (001) GO crystal structure. Fe_3O_4 and GO-Fe_3O_4 showed various Bragg peaks at 30.5° (220), 35.8° (311), 43.4° (400), 57.5° (511), and 63.0° (440). The XRD band at a 2θ of 19.9° corresponded to the (101) PVA crystal structure [14]. Moreover, the GO diffraction peak in the GO-Fe_3O_4 sample at 11° was invisible because the GO content was low (3%). The diffraction peak intensity decreased significantly in the GO-Fe_3O_4-containing QPVA sample. This result implies that addition of GO-Fe_3O_4 particles into the QPVA polymer matrix greatly reduced the percentage of the crystalline domain of the QPVA, as was also shown for the PVA/fumed silica sample [14,40].

For the CL-QPVA and the CL-QPVA/GO-Fe_3O_4 composites prepared with and without the magnetic field, the yield points were 125.4, 22.5, and 41.7 MPa, the failure strain values were 61.4%, 104.7%, and 42.2%, and the Young's moduli were 1.28, 1.14, and 1.07 GPa, respectively (Figure 2b). The Young's moduli of CL-QPVA/GO-Fe_3O_4 composites prepared with and without the magnetic field were lower than that of CL-QPVA. The embedded nanofillers in the CL-QPVA decreased the percentage of crystalline CL-QPVA (Figure 2a) in the composite membrane and hence decreased the modulus. However, the aligned composite showed a significantly higher elongation—at-break value (104.7% vs. 42.2%) than the un-aligned composite. The elongation-at-break indicates that the aligned GO enhanced the membrane's stretchability.

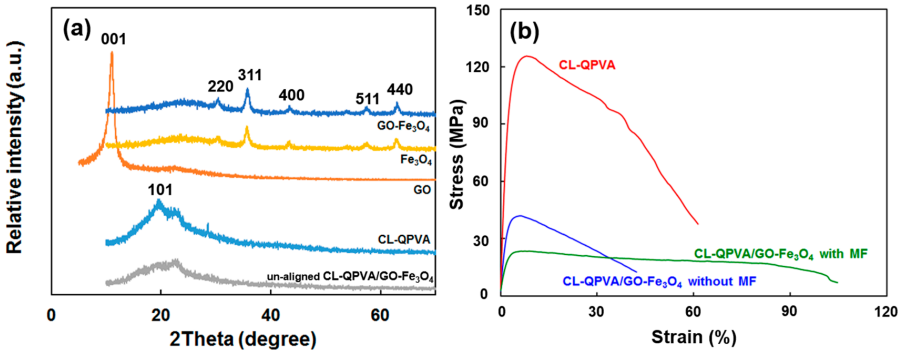

Figure 2. (**a**) X-ray diffraction (XRD) patterns of graphene oxide (GO), iron oxide (Fe_3O_4), graphene oxide-iron oxide (GO-Fe_3O_4), CL-QPVA and un-aligned CL-QPVA/GO-Fe_3O_4 membranes; and (**b**) stress–strain curves of the CL-QPVA and CL-QPVA/GO-Fe_3O_4 composites prepared with and without the magnetic field (MF).

2.3. Methanol Permeability of Quaternized Polyvinyl Alcohol Composite Membranes

Fuel crossover is a primary concern in fuel cell membrane development. Methanol crossover must be reduced to improve the fuel cell performance. Fuel crossover is caused mainly by fuel diffusion due to the concentration gradient inside the membrane and the osmotic drag accompanying the water transport. Decreasing the methanol permeability is essential for designing a high-performance membrane electrolyte for DMAFC applications. We first measured the methanol permeability using the 2 M methanol solution in the source reservoir and found that the methanol permeability of CL-QPVA membrane was 2.57×10^{-7} $cm^2 \cdot s^{-1}$ and 4.51×10^{-6} $cm^2 \cdot s^{-1}$ at 30 °C and 60 °C, respectively, which were significantly lower than the pre-CL pristine QPVA (6.39×10^{-6} $cm^2 \cdot s^{-1}$ at 30 °C) [40]. These data conclude that the methanol permeability was suppressed by post-CL treatment.

During fuel cell operation, the membrane is continuously fed with alkaline fuel, and the membrane was saturated with KOH. Therefore, the methanol permeability through KOH-doped membrane should better reflect the fuel permeation property during cell discharge cycle. For KOH-doped CL-QPVA, the methanol permeability was 1.62×10^{-7} $cm^2 \cdot s^{-1}$ at 30 °C and 1.36×10^{-6} $cm^2 \cdot s^{-1}$ at 60 °C, which was reduced by 37% and 70% from the undoped CL-QPVA. The methanol permeabilities of the KOH-doped CL-QPVA/GO-Fe_3O_4 prepared without the magnetic field treatment were 8.47×10^{-8} $cm^2 \cdot s^{-1}$ and 8.12×10^{-7} $cm^2 \cdot s^{-1}$ at 30 °C and 60 °C, respectively. The methanol permeability of the CL-QPVA/GO-Fe_3O_4 nanocomposite membranes was lower than the permeability of the CL-QPVA membrane (Table 1). This result demonstrated that the incorporation of only 0.1% GO-Fe_3O_4 was effective in blocking methanol penetration and reduced the methanol crossover. The reduction in permeability indicated that addition of GO-Fe_3O_4 could serve as a barrier for methanol transfer. From our previous experience [10], it was found that the addition of nanoparticles impedes methanol molecular diffusion due to a more tortuous transport path.

Table 1. Methanol permeability [a] of KOH-doped CL-QPVA and KOH-doped CL-QPVA/GO-Fe_3O_4 nanocomposites [b] prepared with and without the magnetic field alignment membrane at 30 °C and 60 °C. KOH: Potassium hydroxide; CL-QPVA: Crosslinked quaternized polyvinyl alcohol; GO-Fe_3O_4: Graphene oxide-iron oxide.

Samples	Permeability	
	at 30 °C ($cm^2 \cdot s^{-1}$)	at 60 °C ($cm^2 \cdot s^{-1}$)
CL-QPVA	1.62×10^{-7}	1.36×10^{-6}
Unaligned CL-QPVA/GO-Fe_3O_4	8.47×10^{-8}	8.12×10^{-7}
Aligned CL-QPVA/GO-Fe_3O_4	6.89×10^{-8}	2.96×10^{-7}

Notes: [a] 2 M methanol; [b] Doped with 6 M KOH.

In addition, when a strong external magnetic field was applied, the membrane permeability was reduced further (Table 1) than that without the magnetic field applied. This may be due to the GO-Fe_3O_4 nanofillers having a high apparent aspect ratio [22,37] and being well-aligned by the magnetic field in the CL-QPVA matrix further suppressed the methanol permeation through the membranes. Well-aligned GO-Fe_3O_4 nanofillers created higher tortuosity in the polymer phase for methanol diffusion than the randomly distributed nanofillers. The well-aligned GO-Fe_3O_4 nanofillers effectively hinder methanol permeation.

2.4. Ionic Conductivity of KOH-Doped Quaternized Polyvinyl Alcohol Nanocomposite Membranes

The ionic conductivity values at 30–60 °C were measured for all KOH-doped membranes. The CL-QPVA membrane had a through-plane conductivity of 1.14×10^{-3}–2.62×10^{-3} S·cm^{-1} at 30−60 °C. The in-plane conductivities were 1.17×10^{-3}–2.74×10^{-3} S·cm^{-1} at the same temperatures. The CL-QPVA/GO-Fe_3O_4 composite prepared without the magnetic field showed though-plane conductivity values of 5.51×10^{-3}–5.30×10^{-3} S·cm^{-1} at 30 °C and 60 °C, respectively, along with in-plane conductivities of 5.80×10^{-3}–5.62×10^{-3} S·cm^{-1} at the same temperatures. The aligned CL-QPVA/GO-Fe_3O_4 composite demonstrated through-plane conductivity values of 7.66×10^{-3}–1.01×10^{-2} S·cm^{-1} at 30 °C and 60 °C, respectively, along with in-plane conductivity values of 8.14×10^{-3}−1.08×10^{-2} S·cm^{-1} at the same temperatures. The in-plane conductivities were slightly higher (3%–5%) than the through-plane values in the CL-QPVA film. The un-aligned and aligned CL-QPVA/GO-Fe_3O_4 composites had significantly higher in-plane conductivities (5%–6% and 6%–7%) than the through-plane conductivities, indicating that nanofiller incorporation and reorientation may cause an anisotropic structure in the composite.

We indicated in our previous reports [17,45,46] that the addition of nanofillers to PVA-based membranes resulted in enhanced ionic conductivity due to higher free volume in the polymer matrix. The nanofillers interrupted the polymer crystal structure and increased the polymer amorphous region, which facilitated ion passage. The magnetic field-free sample reflected a similar effect. As the GO-Fe_3O_4 was aligned, more ion transport routes were induced, such as surface diffusion and hopping mechanisms [41]. Therefore, the aligned QPVA exhibited even higher ionic conductivity (Figure 3a). At elevated temperatures, the conductivity increased due to higher ionic mobility (i.e., diffusivity) and the ions could pass through the polymer free volume with ease.

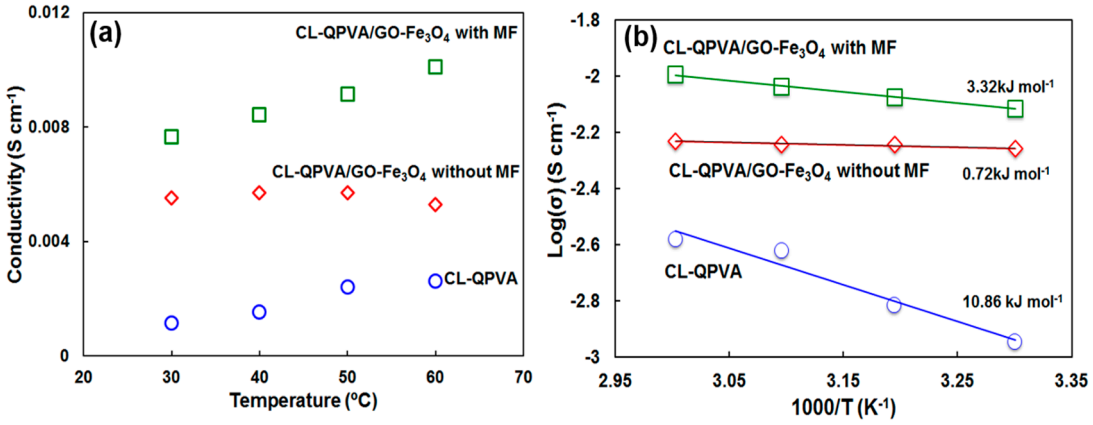

Figure 3. (**a**) original ionic conductivity dependence on temperature; and (**b**) ionic conductivity shown in the Arrhenius relation for KOH-doped CL-QPVA, CL-QPVA/GO-Fe_3O_4 composites prepared with and without the magnetic field. The number indicates the measured activation energy for each membrane.

The temperature dependence of the conductivity can be described using the Arrhenius equation (Figure 3b). The CL-QPVA exhibited an activation energy of 10.86 kJ·mol^{-1}, while the nanocomposites

had lower activation energy levels (<3.5 kJ·mol^{-1}). The differences in activation energy may be due to the different ion conduction mechanisms, which include the Grotthus (hopping) mechanism, bulk diffusion and surface diffusion [41]. Ion conduction through the KOH-doped PVA is based on bulk diffusion through OH^- ions. After quaternization of PVA, the ions could utilize the additional ammonium groups through the hopping mechanism for transport. After the incorporation of the GO-Fe_3O_4 nanofillers, the increased polymer free volume in the polymer matrix allows ions to pass through the QPVA matrix much more easily compared with pristine QPVA [40].

It is noted that KOH doping in PVA or QPVA enhanced membrane integrity. Dragana et al. [47] showed that the KOH-doped PVA was chemically stable in the alkaline environment and considered the KOH treatment a physical crosslinking procedure. Fu et al. [48] confirmed the appearance of a new Fourier transform infra-red spectroscopy (FTIR) peak (at 1573 cm^{-1}) after the PVA was treated with KOH. Qiao et al. [49] also analysed the PVA/PVP membrane after immersion in KOH at different temperatures and found a new bond (CO(–O–K)) in the FTIR spectrum at 1571 cm^{-1}. As other researchers have indicated, we found that the KOH chemical interaction effects make the QPVA and Q-PVA/GO-Fe_3O_4 nanocomposite membranes prepared with and without the magnetic field suitable electrolyte materials for fuel cell applications.

2.5. Direct Methanol Alkaline Fuel Cell Performance of Quaternized Polyvinyl Alcohol Composite Membranes

The DMAFC performances of the prepared membrane electrolytes were first evaluated using 1 M methanol in 6 M KOH. Figure 4 shows the IV curves and power density curves for the DMAFC using the KOH-doped CL-QPVA membrane and CL-QPVA/GO-Fe_3O_4 composites prepared without the magnetic field at 30 °C and 60 °C. Figure 4a illustrates that the DMAFC performance using the CL-QPVA membrane produced a peak power density of 4.5 mW·cm^{-2} and an OCV of 0.68 V at 30 °C. When the temperature was increased to 60 °C, the peak power density increased to 19.4 mW·cm^{-2} and the OCV became 0.83 V. The increased OCV was due to faster catalytic reactions at the electrodes. The higher temperature also facilitated ionic conduction and decreased the electrical resistance of the single cell. Therefore, less ohmic loss was observed at 60 °C than that at 30 °C (Figure 4a). Another cell performance indicator is based on the ratio of the ionic conductivity to the methanol permeability. The ion conductivity/methanol permeability ratio for CL-QPVA were 7.0 × 10^3 and 1.9× 10^3 cm^{-3}·S s at 30 °C and 60 °C, respectively. The overall result was a higher peak power density obtained at 60 °C.

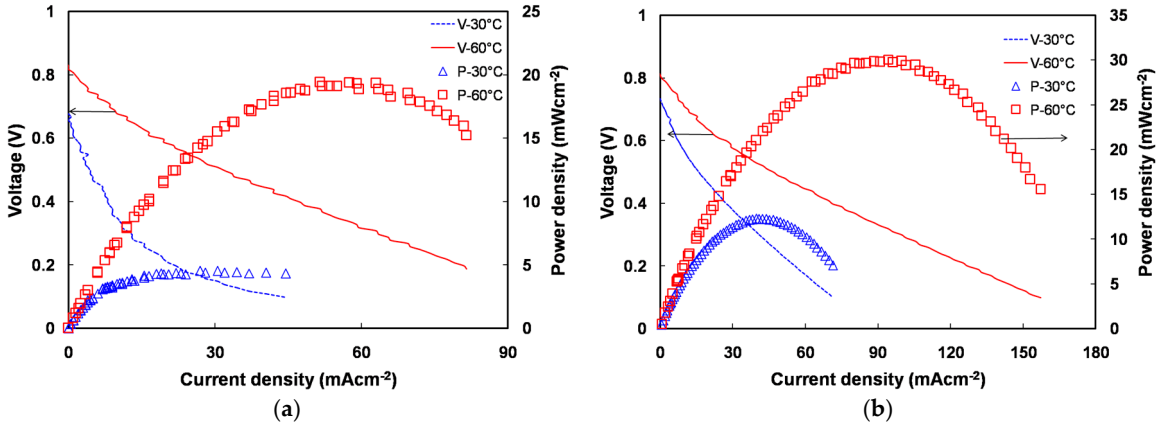

Figure 4. Direct methanol alkaline fuel cell (DMAFC) voltage (left axis) and power density (right axis) as a function of the current density at 30 °C and 60 °C using (**a**) CL-QPVA membrane and (**b**) CL-QPVA/GO-Fe_3O_4 composites prepared without a magnetic field fed with a 1 M methanol anode fuel in 6 M KOH. Cathode: humidified oxygen with a flow rate of 100 mL·min^{-1}. Gas diffusion electrodes (GDEs): catalysts of 6 mg·cm^{-2} Pt-Ru/C for the anode and 5 mg·cm^{-2} Pt/C for the cathode on microporous layer (MPL)-free carbon cloth.

When GO-Fe_3O_4 nanoparticles were added into the QPVA matrix without the magnetic field treatment, the OCV values were 0.72 and 0.80 V at 30 and 60 °C (Figure 4b), respectively. These values were higher than those of the QPVA counterpart, due to the suppressed methanol permeability. The peak power density was 12.3 mW·cm^{-2} at 30 °C and 30 mW·cm^{-2} at 60 °C. Compared to the power density of CL-QPVA, nanofillers' incorporation increased the fuel cell performance significantly. The nanoparticle fillers play a consequential role: nanoparticles provided a blocking barrier for methanol and an ionic transport path to enhance the cell voltage and power density.

Figure 5a,b shows DMAFC performance with 1 M and 2 M methanol in 6 M KOH fuel at 60 °C using CL-QPVA and CL-QPVA/GO-Fe_3O_4 composites prepared without the magnetic field. When the CL-QPVA fuel cell was fed with 1 M and 2 M methanol, the peak power densities were 19.4 mW·cm^{-2} and 22.4 mW·cm^{-2}, respectively (Figure 5a). When the CL-QPVA/GO-Fe_3O_4 composite prepared without the magnetic field was used in the DMAFC, the peak power densities were 30 mW·cm^{-2} and 31.8 mW·cm^{-2} with 1 M and 2 M methanol fuel, respectively. The 2 M methanol fuel had a higher reaction rate and produced more electrical current. Thus, the peak power density was higher for the 2 M methanol fuel than for the 1 M methanol fuel.

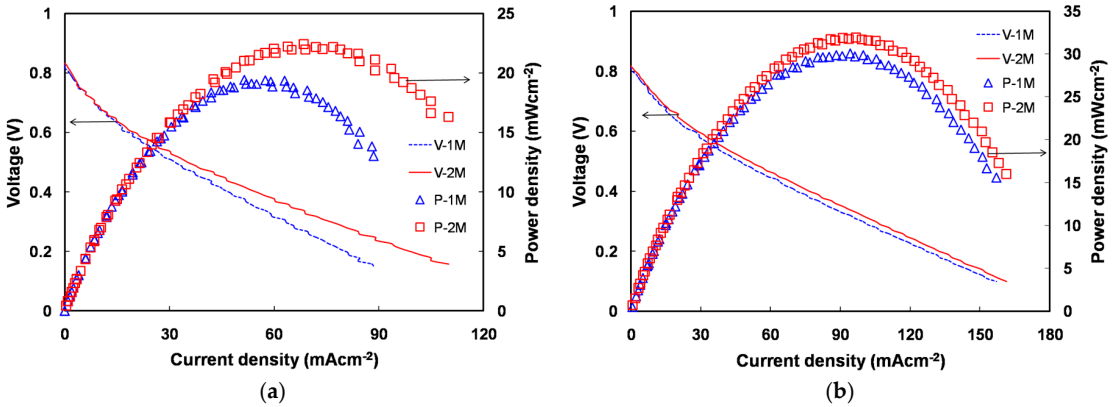

Figure 5. DMAFC performance with different methanol concentrations in 6 M KOH at 60 °C using (**a**) CL-QPVA membrane; (**b**) CL-QPVA/GO-Fe_3O_4 composite prepared without the magnetic field. Cathode: humidified oxygen with a flow rate of 100 mL·min^{-1}. GDEs: catalysts of 6 mg·cm^{-2} Pt-Ru/C for anode and 5 mg·cm^{-2} Pt/C for cathode on MPL-free carbon cloth.

Figure 6 compares the performances of fuel cells assembled with CL-QPVA/GO-Fe_3O_4 composites' electrolyte membranes prepared with and without the magnetic field. The suppressed methanol permeability in the aligned electrolyte improved the OCV due to less mixed potential resulting from methanol crossover. The OCV of CL-QPVA/GO-Fe_3O_4 composite prepared without the magnetic field was 0.82 V and that of CL-QPVA/GO-Fe_3O_4 composite prepared with the magnetic field was 0.85 V. CL-QPVA/GO-Fe_3O_4 composite prepared with the magnetic field had a better maximum power density (55.4 mW·cm^{-2}) than the CL-QPVA/GO-Fe_3O_4 composite prepared without the magnetic field (31.8 mW·cm^{-2}). Employing a magnetic field during the film formation process to arrange the magnetic nanoparticles benefited the fuel cell performance. The higher conductivity and suppressed methanol permeability in the aligned electrolyte led to a lower ohmic loss and produced a higher peak power density than the un-oriented sample.

Furthermore, we fed more concentrated methanol fuel to the DMAFC to compare the power densities using the aligned QPVA composite. The OCV at 1 M, 2 M and 4 M methanol fuels were 0.83, 0.85 and 0.77 V (Figure 7). The 1 M and 2 M methanol resulted in similar OCV values whereas the 4 M fuel had a reduced OCV. The peak power densities with 1 M, 2 M and 4 M methanol fuels were 31.9, 55.4 and 23.5 mW·cm^{-2}, respectively. We have already mentioned that increasing the methanol concentration would also increase the methanol oxidation rate and generate electrical current. However, there is a limit to increasing the methanol concentration. When we raised the methanol concentration

beyond a certain value, the un-reacted methanol would crossover to the cathode. This may result in a mixed potential, catalyst poisoning, and deterioration in the cell performance.

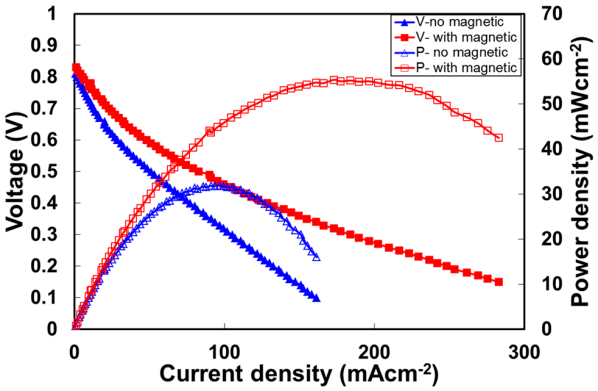

Figure 6. DMAFC voltage (left axis) and power density (right axis) as a function of the current density at 60 °C using CL-QPVA/GO-Fe_3O_4 composites prepared with and without the magnetic field. GDEs: catalysts of 6 mg·cm^{-2} Pt-Ru/C for the anode and 5 mg·cm^{-2} Pt/C for the cathode on MPL-free carbon cloth. Anode fuel: 2 M methanol in 6 M·KOH with a flow rate of 5 mL·min^{-1}, cathode: humidified oxygen with a flow rate of 100 mL·min^{-1}.

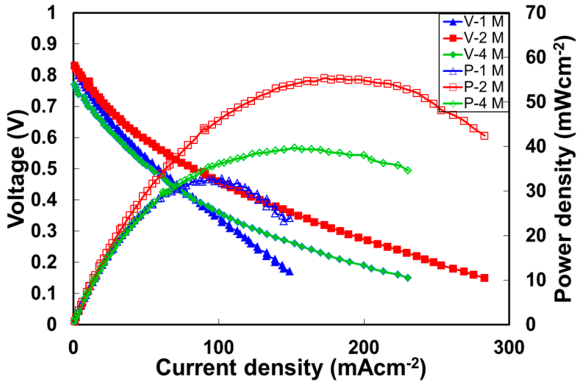

Figure 7. DMAFC performance with different methanol concentrations in 6 M KOH at 60 °C using CL-QPVA/GO-Fe_3O_4 composites prepared with the magnetic field. Cathode: humidified oxygen with a flow rate of 100 mL·min^{-1}. GDEs: catalysts of 6 mg·cm^{-2} Pt-Ru/C for the anode and 5 mg·cm^{-2} Pt/C for the cathode on MPL-free carbon cloth.

3. Materials and Methods

3.1. Materials

Glycidytrimethyl ammonium chloride (GTMAC, 99%), Polyvinyl alcohol (PVA, average molecular weight 89,000–98,000), potassium hydroxide (KOH, 90%), graphite powder, iron (II) chloride tetrahydrate ($FeCl_2 \cdot 4H_2O$, 98%), iron (III) chloride hexahydrate ($FeCl_3 \cdot 6H_2O$, 97%), acetic acid (CH_3CO_2H, 99.85%), ammonium hydroxide (NH_4OH, 28%–30%) and rhodamine B powder (HPLC grade, 95%) were purchased from Sigma-Aldrich (St. Louis, MO, USA). Ethanol (99.9%, HPLC grade), methanol (99.9%, HPLC grade), and *N*,*N*-dimethylformamide (DMF, 99%) were obtained from Acros Organics (Geel, Belgium). Sodium hydroxide solution (NaOH, 50%) was obtained from Showa Chemical Co. Ltd. (Tokyo, Japan). Sulfuric acid solution (H_2SO_4, 95%–98%) was purchased from Scharlab S.L. (Barcelona, Spain). Potassium permanganate powder ($KMnO_4$, 99%) was purchased from Nihon Shiyaku Industries Ltd. (Osaka, Japan). Maleic anhydride (98%) and 4-aminobenzoic acid (*p*-aminobenzoic acid, 99%) were obtained from Alfa Aesar (Lancashire, UK). Tetrahydrofuran (THF)

and acetic anhydride (98%) were purchased from Avantor Performance Materials, Inc. (Center Valley, PA, USA). Sodium acetate was obtained from Shimakyu's Pure Chemicals (Osaka, Japan). Carbon cloth (W0S1002) was obtained from CeTech Co. Ltd. (Taichung, Taiwan). Nafion ionomer solution (5 wt%) was obtained from DuPont (Wilmington, DE, USA). Anode catalyst (Pt-Ru/C, 50%, Pt:Ru = 1:1) was obtained from Tanaka (Tokyo, Japan). Cathode catalyst (Pt/C on carbon, 40%) was from Johnson Matthey (HISPEC^{TM}4000, Royston Hertfordshire, UK). Isopropyl alcohol was purchased from Mallinckrodt Chemicals Ltd. (Chesterfield, UK).

3.2. Preparation of Quaternized Polyvinyl Alcohol and Graphene Oxide-Iron Oxide

The QPVA was quaternized from PVA via reaction with GTMAC and KOH catalyst [40]. The resulting QPVA product was dried at 65 °C in a vacuum oven. The quaternization efficiency was found to be 2.6%. The Fe_3O_4 nanoparticles were prepared by reacting the $FeCl_2/FeCl_3$ mixture with NH_4OH [50]. The product was collected using an external magnet, washed with deionized (D.I.) water, and dried at 40 °C under vacuum for 24 h. GO was prepared using the modified Hummer's method [51]. *p*-Maleimidobenzoic acid (MBA) was prepared as described in the literature [52] and was used as a linker to graft Fe_3O_4 nanoparticles onto GO nanosheets [50].

3.3. Preparation of Quaternized Polyvinyl Alcohol and Quaternized Polyvinyl Alcohol/Graphene Oxide-Iron Oxide Nanocomposite Membrane

Required amounts of QPVA was dissolved in D.I. water to form a 10% solution and stirred for 3 h at 85 °C to synthesize a homogeneous viscous solution. The solution was then poured onto a glass plate. A doctor-blade was applied to produce a uniform thickness of wet QPVA polymeric membrane. Afterwards, the cast wet sample was allowed to gradually evaporate at ambient temperature for 24 h and again dried in a vacuum oven at 60 °C for 6 h.

The dry film was immersed into a cross-linker solution, 10 g GA mixed with 2.85 g HCl and 87.15 g acetone, for 3 h. After the cross-linking process, the membrane was dried at 60 °C in vacuum. The thickness of the resulting dry film was 50 μm. The post-crosslinked membranes were used in most tests. For comparison purposes, a pre-crosslinked QPVA membrane was prepared by mixing the PVA solution and the crosslinker agent (GA), as described in our previous work [40].

To prepare the CL-QPVA/GO-Fe_3O_4 nanocomposite membrane, 0.1 wt% loading of GO-Fe_3O_4 was dispersed in D.I. water and then mixed with QPVA solution at 65 °C for 1 h. The polymer slurry was cast, dried, and crosslinked as previously mentioned. This membrane is referred to as the nanocomposite prepared without the magnetic field (Figure 8a). To orient the GO-Fe_3O_4 particles in the membrane, a magnetic field was added during the membrane drying process. The direction of the magnetic field was perpendicular to the membrane to allow the particles to arrange themselves on the top and bottom of the nanocomposite membrane (Figure 8b).

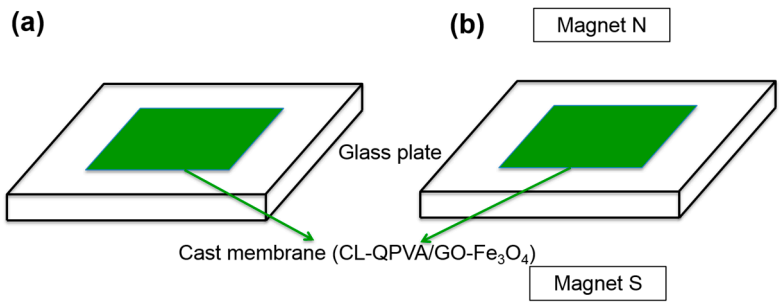

Figure 8. Illustration of CL-QPVA/GO-Fe_3O_4 nanocomposite membranes (**a**) prepared without the magnetic field; and (**b**) prepared with the magnetic field. The magnets are placed above and below the cast film until the membrane solidified.

3.4. Membrane Characterization

The crystallinity properties of the CL-QPVA and CL-QPVA/GO-Fe_3O_4 nanocomposite membrane were measured by XRD (model D5005D, Siemens AG, Munich, Germany). The methanol permeabilities of the CL-QPVA and CL-QPVA/GO-Fe_3O_4 nanocomposite membranes were analysed by using a side-by-side diffusion cell consisting of two-compartment glass reservoirs (source reservoir and receiving reservoir) and the detailed experimental procedure was described in our previous papers [53–55]. The ionic conductivity values of the CL-QPVA and CL-QPVA/GO-Fe_3O_4 nanocomposite membranes in the through-plane direction were measured using the alternating current (AC) impedance method as described in a previous report [49]. The in-plane conductivity was measured using the four-point probe method [55]. The sample mechanical properties were obtained with a texture analyser as described in a previous paper [4].

3.5. Cell Performance Measurement

The CL-QPVA and CL-QPVA/GO-Fe_3O_4 composites prepared with and without the magnetic field were sandwiched between the cathode and anode gas diffusion electrodes (GDEs) to obtain membrane electrode assemblies (MEA). The GDEs were prepared by spraying catalyst (Pt/C or Pt-Ru/C) slurry on microporous layer (MPL) free carbon cloth. The catalyst loads were 5 mg·cm^{-2} Pt/C on the cathode and 6 mg·cm^{-2} Pt-Ru/C on the anode [9]. The final GDE thickness was approximately 0.46 mm and the effective MEA area was 1 cm^2.

The experimental setup was illustrated in our previous work [42,56,57]. The fuel (1 M, 2 M and 4 M methanol in 6 M KOH) was maintained at a predetermined temperature in a thermostatic chamber and recirculated through the anode using a metering pump at a flow rate of 5 mL·min^{-1}. The oxygen cathode feed gas was humidified by passing through a bubbler at a flow rate of 100 cm^3·min^{-1}. The current density (I) and cell potential (V) values of the DMAFCs were recorded on an electrical load (PLZ164 WA electrochemical system, Japan) at a scan rate of 0.01 V·s^{-1}. The power density-current density (P-I) curve was plotted to determine the maximum power density (P_{max}) under a specific operating condition.

4. Conclusions

In this work, Fe_3O_4 nanoparticles were prepared and dispersed on GO nanosheets. The magnetic GO-Fe_3O_4 were embedded into QPVA, and the QPVA was crosslinked with GA to obtain a polymer composite. By applying an external through-plane magnetic field across the thin viscous QPVA/GO-Fe_3O_4 film during drying, the GO-Fe_3O_4 nanosheets in the QPVA membrane were reoriented in the polymer matrix. The magnetic field-reoriented CL-QPVA/GO-Fe_3O_4 membranes possessed higher ionic conductivity and lower methanol permeability than both the un-oriented CL-QPVA/GO-Fe_3O_4 membrane and the CL-QPVA. The reoriented CL-QPVA/GO-Fe_3O_4 nanocomposite exhibited a peak power density of 55.4 mW·cm^{-2} at 60 °C, which was 73.7% higher than that of the nanocomposite without the magnetic field treatment and 147.3% higher than that of the CL-QPVA.

Acknowledgments: Financial support from Chang Gung Memorial University (CMRPD2F0051) and the Ministry of Science and Technology of Taiwan (MOST-103-2815-C-182-023-E and MOST-103-2221-E-182-064-MY3) is gratefully acknowledged.

Author Contributions: Jia-Shuin Lin, and Shingjiang Jessie Lue conceived and designed the experiments, measured the fuel cell performance and performed all data analysis; Jia-Shuin Lin, Wei-Ting Ma, and Shingjiang Jessie Lue wrote the paper; Bor-Chern Yu, Li-Wei Teng and Yi-Chun Wang contributed to the preparation of the QPVA polymer and composite characterization; Chao-Ming Shih and Kong-Wei Cheng conducted the in-plane ionic conductivity measurement; Fang-Chyou Chiu assisted with mechanical property measurements. All authors examined and approved the final manuscript.

Conflicts of Interest: The authors declare no conflict of interest.

References

1. Hardman, S.; Chandan, A.; Steinberger-Wilckens, R. Fuel cell added value for early market applications. *J. Power Sources* **2015**, *287*, 297–306. [CrossRef]
2. Neburchilov, V.; Martin, J.; Wang, H.; Zhang, J. A review of polymer electrolyte membranes for direct methanol fuel cells. *J. Power Sources* **2007**, *169*, 221–238. [CrossRef]
3. Dyer, C.K. Fuel cells for portable applications. *J. Power Sources* **2002**, *106*, 31–34. [CrossRef]
4. Liao, G.M.; Li, P.C.; Lin, J.S.; Ma, W.T.; Yu, B.C.; Li, H.Y.; Liu, Y.L.; Yang, C.C.; Shih, C.M.; Lue, S.J. Highly conductive quasi-coaxial electrospun quaternized polyvinyl alcohol nanofibers and composite as high-performance solid electrolytes. *J. Power Sources* **2016**, *304*, 136–145. [CrossRef]
5. Li, P.C.; Liao, G.M.; Kumar, S.R.; Shih, C.M.; Yang, C.C.; Wang, D.M.; Lue, S.J. Fabrication and characterization of chitosan nanoparticle-incorporated quaternized poly(vinyl alcohol) composite membranes as solid electrolytes for direct methanol alkaline fuel cells. *Electrochim. Acta* **2016**, *187*, 616–628. [CrossRef]
6. Varcoe, J.R.; Atanassov, P.; Dekel, D.R.; Herring, A.M.; Hickner, M.A.; Kohl, P.A.; Kucernak, A.R.; Mustain, W.E.; Nijmeijer, K.; Scott, K.; et al. Anion-exchange membranes in electrochemical energy systems. *Energy Environ. Sci.* **2014**, *7*, 3135–3191. [CrossRef]
7. Kumar, S.R.; Juan, C.H.; Liao, G.M.; Lin, J.S.; Yang, C.C.; Ma, W.T.; You, J.H.; Lue, S.J. Fumed silica nanoparticles incorporated in quaternized poly (vinyl alcohol) nanocomposite membrane for enhanced power densities in direct alcohol alkaline fuel cells. *Energies* **2015**, *9*, 15. [CrossRef]
8. Wu, J.F.; Lo, C.F.; Li, L.Y.; Li, H.Y.; Chang, C.M.; Liao, K.S.; Hu, C.C.; Liu, Y.L.; Lue, S.J. Thermally stable polybenzimidazole/carbon nano-tube composites for alkaline direct methanol fuel cell applications. *J. Power Sources* **2014**, *246*, 39–48. [CrossRef]
9. Li, L.Y.; Yu, B.C.; Shih, C.M.; Lue, S.J. Polybenzimidazole membranes for direct methanol fuel cell: Acid-doped or alkali-doped? *J. Power Sources* **2015**, *287*, 386–395. [CrossRef]
10. Lo, C.F.; Wu, J.F.; Li, H.Y.; Hung, W.S.; Shih, C.M.; Hu, C.C.; Liu, Y.L.; Lue, S.J. Novel polyvinyl alcohol nanocomposites containing carbon nano-tubes with Fe_3O_4 pendants for alkaline fuel cell applications. *J. Membr. Sci.* **2013**, *444*, 41–49. [CrossRef]
11. Tripković, A.V.; Popović, K.D.; Grgur, B.N.; Blizanac, B.; Ross, P.N.; Marković, N.M. Methanol electrooxidation on supported Pt and PtRu catalysts in acid and alkaline solutions. *Electrochim. Acta* **2002**, *47*, 3707–3714. [CrossRef]
12. Lu, S.; Pan, J.; Huang, A.; Zhuang, L.; Lu, J. Alkaline polymer electrolyte fuel cells completely free from noble metal catalysts. *Proc. Natl. Acad. Sci. USA* **2008**, *105*, 20611–20614. [CrossRef]
13. Huang, C.Y.; Lin, J.S.; Pan, W.H.; Shih, C.M.; Liu, Y.L.; Lue, S.J. Alkaline direct ethanol fuel cell performance using alkali-impregnated polyvinyl alcohol/functionalized carbon nano-tube solid electrolytes. *J. Power Sources* **2016**, *303*, 267–277. [CrossRef]
14. Lue, S.J.; Mahesh, K.P.O.; Wang, W.T.; Chen, J.Y.; Yang, C.C. Permeant transport properties and cell performance of potassium hydroxide doped poly(vinyl alcohol)/fumed silica nanocomposites. *J. Membr. Sci.* **2011**, *367*, 256–264. [CrossRef]
15. Yang, C.C.; Chiu, S.J.; Chien, W.C.; Chiu, S.S. Quaternized poly(vinyl alcohol)/alumina composite polymer membranes for alkaline direct methanol fuel cells. *J. Power Sources* **2010**, *195*, 2212–2219. [CrossRef]
16. Ma, W.T.; Wang, Y.C.; Yu, B.C.; Teng, L.W.; Shih, C.M.; Tsai, S.W.; Liu, Y.L.; Lue, S.J. Magnetic field-assisted alignment of graphene oxide nanosheets in polymer matrix for enhancing ionic conduction. *J. Membr. Sci.* **2016**, in revision.
17. Lue, S.J.; Lee, D.T.; Chen, J.Y.; Chiu, C.H.; Hu, C.C.; Jean, Y.C.; Lai, J.Y. Diffusivity enhancement of water vapor in poly(vinyl alcohol)-fumed silica nano-composite membranes: Correlation with polymer crystallinity and free-volume properties. *J. Membr. Sci.* **2008**, *325*, 831–839. [CrossRef]
18. Yuan, T.; Pu, L.; Huang, Q.; Zhang, H.; Li, X.; Yang, H. An effective methanol-blocking membrane modified with graphene oxide nanosheets for passive direct methanol fuel cells. *Electrochim. Acta* **2014**, *117*, 393–397. [CrossRef]
19. Yang, C.C.; Chiu, S.J.; Lee, K.T.; Chien, W.C.; Lin, C.T.; Huang, C.A. Study of poly(vinyl alcohol)/titanium oxide composite polymer membranes and their application on alkaline direct alcohol fuel cell. *J. Power Sources* **2008**, *184*, 44–51. [CrossRef]

20. Movil, O.; Frank, L.; Staser, J.A. Graphene oxide-polymer nanocomposite anion-exchange membranes. *J. Electrochem. Soc.* **2015**, *162*, F419–F426. [CrossRef]
21. Nair, R.R.; Wu, H.A.; Jayaram, P.N.; Grigorieva, I.V.; Geim, A.K. Unimpeded permeation of water through helium-leak-tight graphene-based membranes. *Science* **2012**, *335*, 442–444. [CrossRef] [PubMed]
22. Lue, S.J.; Pai, Y.L.; Shih, C.M.; Wu, M.C.; Lai, S.M. Novel bilayer well-aligned Nafion/graphene oxide composite membranes prepared using spin coating method for direct liquid fuel cells. *J. Membr. Sci.* **2015**, *493*, 212–223. [CrossRef]
23. Vadivel Murugan, A.; Muraliganth, T.; Manthiram, A. Rapid, facile microwave-solvothermal synthesis of graphene nanosheets and their polyaniline nanocomposites for energy strorage. *Chem. Mater.* **2009**, *21*, 5004–5006. [CrossRef]
24. Zhao, G.; Li, J.; Ren, X.; Chen, C.; Wang, X. Few-layered graphene oxide nanosheets as superior sorbents for heavy metal ion pollution management. *Environ. Sci. Technol.* **2011**, *45*, 10454–10462. [CrossRef] [PubMed]
25. Marcano, D.C.; Kosynkin, D.V.; Berlin, J.M.; Sinitskii, A.; Sun, Z.; Slesarev, A.; Alemany, L.B.; Lu, W.; Tour, J.M. Improved synthesis of graphene oxide. *ACS Nano* **2010**, *4*, 4806–4814. [CrossRef] [PubMed]
26. Alabadi, A.; Razzaque, S.; Dong, Z.; Wang, W.; Tan, B. Graphene oxide-polythiophene derivative hybrid nanosheet for enhancing performance of supercapacitor. *J. Power Sources* **2016**, *306*, 241–247. [CrossRef]
27. Pandey, R.P.; Shahi, V.K. Sulphonated imidized graphene oxide (SIGO) based polymer electrolyte membrane for improved water retention, stability and proton conductivity. *J. Power Sources* **2015**, *299*, 104–113. [CrossRef]
28. Yuan, M.; Erdman, J.; Tang, C.; Ardebili, H. High performance solid polymer electrolyte with graphene oxide nanosheets. *RSC Adv.* **2014**, *4*, 59637–59642. [CrossRef]
29. Wang, L.S.; Lai, A.N.; Lin, C.X.; Zhang, Q.G.; Zhu, A.M.; Liu, Q.L. Orderly sandwich-shaped graphene oxide/Nafion composite membranes for direct methanol fuel cells. *J. Membr. Sci.* **2015**, *492*, 58–66. [CrossRef]
30. Beydaghi, H.; Javanbakht, M. Aligned nanocomposite membranes containing sulfonated graphene oxide with superior ionic conductivity for direct methanol fuel cell application. *Ind. Eng. Chem. Res.* **2015**, *28*, 7028–7037. [CrossRef]
31. Aricò, A.S.; Baglio, V.; Antonucci, V.; Nicotera, I.; Oliviero, C.; Coppola, L.; Antonucci, P.L. An NMR and SAXS investigation of DMFC composite recast Nafion membranes containing ceramic fillers. *J. Membr. Sci.* **2006**, *270*, 221–227. [CrossRef]
32. Zhao, Y.; Fu, Y.; Hu, B.; Lv, C. Quaternized graphene oxide modified ionic cross-linked sulfonated polymer electrolyte composite proton exchange membranes with enhanced properties. *Solid State Ion.* **2016**, *294*, 43–53. [CrossRef]
33. Nicotera, I.; Angjeli, K.; Coppola, L.; Aricò, A.S.; Baglio, V. NMR and electrochemical investigation of the transport properties of methanol and water in Nafion and clay-nanocomposites membranes for DMFCs. *Membranes* **2012**, *2*, 325–345. [CrossRef] [PubMed]
34. Yang, C.C. Alkaline direct methanol fuel cell based on a novel anion-exchange composite polymer membrane. *J. Appl. Electrochem.* **2012**, *42*, 305–317. [CrossRef]
35. Nicotera, I.; Simari, C.; Coppola, L.; Zygouri, P.; Gournis, D.; Brutti, S.; Minuto, F.D.; Aricò, A.S.; Sebastian, D.; Baglio, V. Sulfonated graphene oxide platelets in Nafion nanocomposite membrane: Advantages for application in direct methanol fuel cells. *J. Phys. Chem. C* **2014**, *118*, 24357–24368. [CrossRef]
36. Paneri, A.; He, Y.; Ehlert, G.; Cottrill, A.; Sodano, H.; Pintauro, P.; Moghaddam, S. Proton selective ionic graphene-based membrane for high concentration direct methanol fuel cells. *J. Membr. Sci.* **2014**, *467*, 217–225. [CrossRef]
37. Lin, C.W.; Lu, Y.S. Highly ordered graphene oxide paper laminated with a Nafion membrane for direct methanol fuel cells. *J. Power Sources* **2013**, *237*, 187–194. [CrossRef]
38. Choi, B.G.; Huh, Y.S.; Park, Y.C.; Jung, D.H.; Hong, W.H.; Park, H. Enhanced transport properties in polymer electrolyte composite membranes with graphene oxide sheets. *Carbon* **2012**, *50*, 5395–5402. [CrossRef]
39. Kumar, R.; Xu, C.; Scott, K. Graphite oxide/Nafion composite membranes for polymer electrolyte fuel cells. *RSC Adv.* **2012**, *2*, 8777–8782. [CrossRef]
40. Liao, G.M.; Yang, C.C.; Hu, C.C.; Pai, Y.L.; Lue, S.J. Novel quaternized polyvinyl alcohol/quaternized chitosan nano-composite as an effective hydroxide-conducting electrolyte. *J. Membr. Sci.* **2015**, *485*, 17–29. [CrossRef]

41. Peckham, T.J.; Holdcroft, S. Structure-morphology-property relationships of non-perfluorinated proton-conducting membranes. *Adv. Mater.* **2010**, *22*, 4667–4690. [CrossRef] [PubMed]
42. Wang, B.Y.; Lin, H.K.; Liu, N.Y.; Mahesh, K.P.O.; Lue, S.J. Cell performance modeling of direct methanol fuel cells using proton-exchange solid electrolytes: Effective reactant diffusion coefficients in porous diffusion layers. *J. Power Sources* **2013**, *227*, 275–283. [CrossRef]
43. Guo, H.; Wyart, Y.; Perot, J.; Nauleau, F.; Moulin, P. Magnetic nanoparticles for UF membrane integrity: Industrial scale. *Membr. Water Treat.* **2011**, *2*, 1–11.
44. Xiong, Y.; Fang, J.; Zeng, Q.H.; Liu, Q.L. Preparation and characterization of cross-linked quaternized poly(vinyl alcohol) membranes for anion exchange membrane fuel cells. *J. Membr. Sci.* **2008**, *311*, 319–325. [CrossRef]
45. Lue, S.J.; Wang, W.T.; Mahesh, K.P.O.; Yang, C.C. Enhanced performance of a direct methanol alkaline fuel cell (DMAFC) using a polyvinyl alcohol/fumed silica/KOH electrolyte. *J. Power Sources* **2010**, *195*, 7991–7999. [CrossRef]
46. Lue, S.J.; Pan, W.H.; Chang, C.M.; Liu, Y.L. High-performance direct methanol alkaline fuel cells using potassium hydroxide-impregnated polyvinyl alcohol/carbon nano-tube electrolytes. *J. Power Sources* **2012**, *202*, 1–10. [CrossRef]
47. Dragana, I.M.P.; Zugic, L.; Nikolic, V.M.; Maslovara, S.L.; Kaninski, M.P.M. Enhanced performance of the solid alkaline fuel cell using PVA-KOH membrane. *Int. J. Electrochem. Sci.* **2013**, *8*, 949–957.
48. Fu, J.; Qiao, J.; Lv, H.; Ma, J.; Yuan, X.Z.; Wang, H. Alkali doped poly(vinyl alcohol) (PVA) for anion-exchange membrane fuel cells: Ionic conductivity, chemical stability and FT-IR characterizations. *ECS Trans.* **2010**, *25*, 15–23.
49. Qiao, J.; Fu, J.; Lin, R.; Ma, J.; Liu, J. Alkaline solid polymer electrolyte membranes based on structurally modified PVA/PVP with improved alkali stability. *Polymer* **2010**, *51*, 4850–4859. [CrossRef]
50. Li, H.Y.; Chang, C.M.; Hsu, K.Y.; Liu, Y.L. Poly(lactide)-functionalized and Fe_3O_4 nanoparticle-decorated multiwalled carbon nanotubes for preparation of electrically-conductive and magnetic poly(lactide) films and electrospun nanofibers. *J. Mater. Chem.* **2012**, *22*, 4855. [CrossRef]
51. Shen, X.; Jiang, L.; Ji, Z.; Wu, J.; Zhou, H.; Zhu, G. Stable aqueous dispersions of graphene prepared with hexamethylenetetramine as a reductant. *J. Colloid Interface Sci.* **2011**, *354*, 493–497. [CrossRef] [PubMed]
52. Annunziato, M.E.; Patel, U.S.; Ranade, M.; Palumbo, P.S. p-Maleimidophenylisocyanate: A novel heterobifunctional linker for hydroxyl to thiol coupling. *Bioconjugate Chem.* **1993**, *4*, 212–218. [CrossRef]
53. Lue, S.J.; Chien, C.F.; Mahesh, K.P.O. Pervaporative concentration of ethanol–water mixtures using heterogeneous polydimethylsiloxane (PDMS) mixed matrix membranes. *J. Membr. Sci.* **2011**, *384*, 17–26. [CrossRef]
54. Lue, S.J.; Liaw, T.-H. Separation of xylene mixtures using polyurethane-zeolite composite membranes. *Desalination* **2006**, *193*, 137–143. [CrossRef]
55. Lue, S.J.; Shih, T.S.; Wei, T.C. Plasma modification on a Nafion membrane for direct methanol fuel cell applications. *Korean J. Chem. Eng.* **2006**, *23*, 441–446. [CrossRef]
56. Cheng, K.W.; Huang, C.M.; Pan, G.T.; Chang, W.S.; Lee, T.C.; Yang, T.C.K. The physical properties and photoresponse of $AgIn_5S_8$ polycrystalline film electrodes fabricated by chemical bath deposition. *J. Photochem. Photobiol. A Chem.* **2007**, *190*, 77–87. [CrossRef]
57. Wang, B.Y.; Tseng, C.K.; Shih, C.M.; Pai, Y.L.; Kuo, H.P.; Lue, S.J. Polytetrafluoroethylene (PTFE)/silane cross-linked sulfonated poly(styrene-ethylene/butylene-styrene) (sSEBS) composite membrane for direct alcohol and formic acid fuel cells. *J. Membr. Sci.* **2014**, *464*, 43–54. [CrossRef]